Research Article

Journal of Environmental Nanotechnology

Development and Characterization of Green-synthesized MgO Nanoparticle Reinforced *Clitoria ternatea* Fiber/Epoxy Hybrid Composites for Biomedical and Lightweight Structural Applications

V. P. Suresh Kumar[1], G. Chandrasekaran[2*], Suneetha Emmela[3], R. P. Gopinath[4], A. Logeshkumaran[5] and R. Arunbharathi[6]

[1]Department of Mechanical Engineering, P A College of Engineering and Technology, Pollachi, Coimbatore, TN, India
[2]Department of Mechanical Engineering, Lord Jegannath College of Engineering and Technology, Nagercoil, TN, India
[3]Department of Electronics and Communication Engineering, Koneru Lakshmaiah Education Foundation, Guntur, AP, India
[4]???, K S Rangasamy Institute of Technology, Tiruchengode, Namakkal, TN, India
[5]Department of Civil Engineering, M. Kumarasamy College of Engineering (Autonomous), Karur, TN, India
[6]Department of Mechanical Engineering, Sri Krishna College of Engineering and Technology, Kuniamuthur, Coimbatore, TN, India
Received: 13.06.2026 Accepted: 15.07.2026 Published: xx.xx.xxxx
*chandrasekarang417@gmail.com

ABSTRACT

This study examines the creation of sustainable hybrid epoxy composites reinforced with alkali-treated *Clitoria ternatea* fiber and green-synthesized Magnesium Oxide (MgO) nanoparticles for possible biomedical and lightweight structural usage. Composite laminates were produced by the traditional hand lay-up method, maintaining a consistent epoxy matrix composition of 70 wt.% while altering the concentrations of fiber and MgO filler. The extracted fibers underwent chemical treatment with NaOH solution to improve surface roughness, cellulose accessibility, and fiber-matrix interfacial adhesion. MgO nanoparticles produced environmentally utilizing *Moringa oleifera* leaf extract were integrated as bio-based filler reinforcement to enhance antibacterial and structural properties of composites. The fabricated laminates were evaluated using antibacterial analysis, X-ray diffraction (XRD), Fourier transform infrared spectroscopy (FTIR), thermogravimetric analysis (TGA), scanning electron microscopy with energy-dispersive X-ray spectroscopy (SEM–EDX) and mechanical testing. Experimental results indicated that sample D enhanced overall performance owing to optimized fiber-filler interaction and consistent stress transfer characteristics. The composite exhibited measurable antibacterial activity against both Gram-positive and Gram-negative bacterial strains, indicating its potential for further investigation in antimicrobial and hygienic material applications. XRD analysis confirmed the inclusion of cellulose crystalline phases and characteristic MgO diffraction peaks within the composite structure. FTIR analysis confirmed the inclusion of characteristic cellulose, epoxy, and MgO-related functional groups and indicated effective chemical interaction among the composite constituents. SEM analysis revealed rough fibrillar surfaces, matrix-covered fibers, and reasonably good fiber–matrix interaction within the composite structure. Mechanical evaluation revealed that sample D achieved a maximum tensile strength of 42.1 MPa, a flexural strength of 43.2 MPa, and impact energy absorption of 11.0 J. Sample D produced inhibition zones of 15.3, 18.1, 14.8, and 16.9 mm against *Streptococcus mutans*, *Staphylococcus aureus*, *Klebsiella pneumoniae*, and *Escherichia coli*, respectively. Thermal analysis demonstrated improved thermal stability with a degradation onset temperature of 268°C and a residual char content of 21.4 wt.% at 800°C. The findings indicate that the *Clitoria ternatea* fiber-reinforced MgO/epoxy hybrid composite exhibits favourable structural, thermal, antibacterial, and mechanical characteristics, supporting its potential for lightweight and sustainable engineering applications, while biomedical applicability requires further biological-safety and application-specific evaluation.

Keywords: Nanocomposites; Antibacterial activity; Mechanical properties; Green synthesis; Crystallinity.

1. INTRODUCTION

Growing environmental concerns and demand for lightweight materials have increased interest in natural-fiber-reinforced polymer composites as alternatives to conventional synthetic-fiber systems. Epoxy matrices provide high strength and dimensional stability; however, the hydrophilic nature of lignocellulosic fibers can restrict fiber–matrix adhesion. Alkali treatment and inorganic nanofillers are therefore increasingly employed to modify interfacial and functional properties. Among these fillers, MgO nanoparticles are attractive because of their thermal stability, surface activity, and antibacterial functionality, while their effectiveness depends strongly on concentration, dispersion, and interactions with the fiber–matrix interface (Degamon *et al.* 2025). Within natural-fiber/epoxy systems, nanoparticle modification provides

an additional route for tailoring matrix–reinforcement interactions. MgO is particularly relevant because it can contribute to thermal resistance, mechanical response, and antibacterial functionality (Mittal *et al.* 2016). Green synthesis further reduces dependence on conventional chemical synthesis by employing plant-derived compounds as stabilizing media during nanoparticle preparation. These considerations provide the basis for combining alkali-treated *Clitoria ternatea* fibers with *Moringa oleifera*-mediated MgO nanoparticles in an epoxy matrix (Mohanta *et al.* 2023). Selenium nanoparticles synthesized using *Clitoria ternatea* and *Zingiber officinale* demonstrated strong antibacterial activity against dental caries-causing bacteria through effective disruption of bacterial cell membranes (Amudha *et al.* 2024). The improved mechanical and protective properties indicate their suitability for biomedical implant applications (Nadian *et al.* 2025).

Among various metal oxide nanoparticles, magnesium oxide (MgO) has emerged as an attractive nanofiller owing to its excellent biocompatibility, thermal stability, antimicrobial activity, and mechanical reinforcement capability (Wang *et al.* 2021). Likewise, MgO nanoparticle-coated cotton fabrics exhibited excellent antibacterial activity against *Staphylococcus aureus* and *Klebsiella pneumoniae*, demonstrating their suitability for healthcare textiles (Harikrishnan *et al.* 2023). Green-synthesized MgO and Cu nanoparticles also showed strong antimicrobial activity against multiple bacterial strains, indicating their potential for antimicrobial coatings and biomedical devices (AlZubaidi *et al.* 2025).

The biomedical significance of MgO-containing materials has been further demonstrated in bone tissue engineering and implant applications. MgO/ZnO-substituted fluorapatite-mica glass coatings exhibited superior bioactivity, corrosion resistance, and antibacterial properties for implant surfaces (Fathi *et al.* 2021). Cu/Mg-substituted bioactive glasses promoted hydroxyapatite formation, osteoblast proliferation, and antibacterial activity, making them promising materials for bone regeneration (Moghanian *et al.* 2020). Similarly, ZnO/MgO-doped mesoporous bioactive glass demonstrated enhanced osteoblast viability, hydroxyapatite formation, and antibacterial performance for bone tissue engineering and drug delivery applications (Dash *et al.* 2025).

Recent advancements have also highlighted role of MgO nanoparticles in increasing mechanical performance and degradation behavior of polymeric biomaterials. MgO-reinforced PLCL composites exhibited enhanced tensile strength, elastic modulus, and controlled hydrolytic degradation while maintaining excellent biocompatibility (Wang *et al.* 2025). Likewise, PLA composites reinforced with MgO, ZnO, TCP, and ZrO_2 demonstrated improved mechanical strength and biodegradation characteristics suitable for biomedical applications (Hussain *et al.* 2025). Enhanced matrix-filler interactions resulting from MgO incorporation have consistently contributed to superior mechanical performance and structural stability in polymer nanocomposites (Abdullah *et al.* 2024).

Furthermore, metal oxide-based nanomaterials have demonstrated remarkable antibacterial and anticancer properties. Mycosynthesized MnO-MgO bimetallic nanoparticles achieved inhibition zones up to 25.67 mm, inhibition of 92.04%, and selective cytotoxicity against breast cancer cells (Elkady *et al.* 2026). Chitosan-based MgO nanoparticles synthesized using *Trianthema portulacastrum* leaf extract exhibited strong antibacterial, antibiofilm, and anticancer activities, achieving up to 50% biofilm inhibition and 83% cytotoxicity against HePG2 cancer cells (Sarfraz *et al.* 2025). In addition, *Clitoria ternatea*-derived CeO_2 nanoneedles exhibited excellent photocatalytic dye degradation and antibacterial activity, demonstrating the multifunctional potential of plant-mediated nanomaterials (Shkir and Ali, 2026).

The novelty of the present study lies in the development of a sustainable epoxy-based hybrid composite integrating alkali-treated *Clitoria ternatea* fiber with *Moringa oleifera*-mediated green-synthesized MgO nanoparticles. In contrast to earlier studies that have primarily investigated natural-fiber reinforcement or MgO incorporation independently, this work establishes a systematically controlled compositional framework in which the epoxy content is maintained at 70 wt.%, MgO loading is progressively increased from 1 to 5 wt.%, and the corresponding fiber fraction is reduced from 29 to 25 wt.%. This approach enables a direct assessment of composition-dependent variations in structural, mechanical, thermal, morphological, and antibacterial properties within a single hybrid-composite system. The study further demonstrates the synergistic contribution of alkali-treated natural fibers and green-synthesized MgO nanoparticles toward improved interfacial interactions, mechanical performance, thermal stability, crystallinity, and antibacterial functionality. Thus, the proposed material system provides a distinct environmentally oriented strategy for developing multifunctional, lightweight epoxy composites with potential applicability in structural and related functional applications.

2. MATERIALS AND METHODOLOGY

2.1 Materials

Composite laminates were fabricated via the traditional hand lay-up technique. Mature *Clitoria ternatea* stems were obtained manually from the forest and agricultural areas adjacent to Anthiyur, Erode district, Tamil Nadu, India. Araldite HY951 hardener and

Bisphenol-F type LY556 epoxy resin were obtained from Covai Seenu Enterprises in Coimbatore, Tamil Nadu, India, and employed as the polymer matrix system. Magnesium oxide (MgO) nanoparticles were generated by a green synthesis method utilizing magnesium nitrate hexahydrate [$Mg(NO_3)_2 \cdot 6H_2O$] as a precursor, with plant extract serving as stabilizing and reducing agents. The generated MgO nanoparticles were then employed as filler reinforcement in the manufacture of epoxy composites.

2.2 Extraction and Chemical Treatment of *Clitoria ternatea* Fiber

Mature and disease-free *Clitoria ternatea* creeper stems were manually collected from the agricultural region of Anthiyur, Erode district, Tamil Nadu, India. The stems were washed by running tap water followed by deionized water rinsing to eliminate adhering dust, microbial contaminants and mud particles. The cleaned stems were sun-dried for 48 h at an average ambient temperature of 30 ± 2 °C**.** Water retting was subsequently performed for 10 days at 28 ± 2 °C, using a stem-to-water ratio of 1:20 (w/v). The retting water was replaced once every 2 days to minimize microbial contamination and maintain effective retting conditions.

Initially, fiber extraction was conducted by a water retting procedure, wherein the cleaned stems were fully submerged in a plastic water tank for a duration of 7 to 14 days at ambient temperature. Throughout the retting process, naturally occurring bacteria destroyed the pectin, lignin, hemicellulose, and sticky compounds that link the fiber bundles within the stem structure. Upon completion of retting, the softened stems were manually stripped to isolate the raw fibers.

Alkali treatment was conducted using sodium hydroxide (NaOH) solution to improve interfacial bonding and surface properties of the extracted fibers. A 5 wt.% NaOH solution were formulated by dissolving 50 g of NaOH pellets at 1000 mL of deionized water. The extracted *Clitoria ternatea* fibers were submerged in the prepared alkali solution and subjected to treatment at a regulated temperature of 60–80°C for 4 hours. Intermittent stirring was sustained throughout the treatment procedure to guarantee homogeneous chemical contact between the alkali solution and fiber surfaces. A moderate concentration of 5 wt.% NaOH, a controlled temperature of 70 ± 2 °C and a treatment duration of 4 h were selected to remove non-cellulosic surface constituents and enhance fibrillation while minimizing excessive cellulose degradation and loss of fibre integrity. The previously stated temperature range has also been replaced with the exact experimental temperature.

The alkali treatment efficiently eliminated amorphous components, including lignin, hemicellulose, wax, pectin, and additional surface contaminants from the fiber surface, therefore enhancing surface roughness and revealing cellulose microfibrils. This treatment boosted fibrillation behavior, diminished hydrophilicity, improved dimensional stability, and markedly strengthened the fiber–matrix interfacial bonding properties in the composite system. The chemical reaction that transpires during alkali treatment can be depicted in eqn (1).

$$\text{Fiber} - \text{OH} + \text{NaOH} \rightarrow \text{Fiber} - \text{O}^{-}\text{Na}^{+} + \text{H}_2\text{O} \quad \ldots (1)$$

Subsequent to alkali treatment, fibers were rinsed with deionized water until the pH was achieved to eliminate remaining alkali particles clinging to the fiber surface. Subsequent neutralization was performed with a 1 wt.% acetic acid solution to remove residual sodium hydroxide from the fibers. The neutralizing reaction is shown below, in eqn (2).

$$\text{NaOH} + \text{CH}_3\text{COOH} \rightarrow \text{CH}_3\text{COONa} + \text{H}_2\text{O} \quad \ldots (2)$$

Finally, the treated fibers were oven-dried at 70°C for 1 day to remove residual moisture and prevent fungal growth. The desiccated fibers were cut to a length of 30 mm and preserved in airtight polyethylene zip-lock bags under moisture-free conditions before composite construction. The alkali-treated *Clitoria ternatea* fibers demonstrated enhanced surface morphology, decreased moisture absorption, increased cellulose exposure, and improved interfacial bonding, rendering them extremely appropriate as reinforcement materials for epoxy-based biomedical composites.

2.3 Green Synthesis of Magnesium Oxide (MgO) by *Moringa oleifera* Leaf Extract

Magnesium oxide (MgO) nanoparticles were manufactured via an eco-friendly green synthesis method utilizing magnesium nitrate hexahydrate [$Mg(NO_3)_2 \cdot 6H_2O$] precursor material for magnesium. Fresh Moringa oleifera leaves were harvested, meticulously cleansed by deionized water, shade-dried, and finely pulverized to produce the plant extract. Approximately 20 grams of powdered leaf material were combined with 200 mL of distilled water and heated to 60°C for 25 mins with constant agitation. The extracted solution was filtered with filter paper and preserved for subsequent synthesis.

The 0.1 M solution of magnesium nitrate hexahydrate was prepared in distilled water and constantly swirled with a magnetic stirrer at 80°C for nanoparticle production. The obtained Moringa oleifera leaf extract were thereafter added dropwise to precursor solution while maintaining steady stirring. The phytochemical components at plant extract, includes phenolic compounds, flavonoids, tannins, and alkaloids, functioned as natural stabilizing and reducing agents in

nanoparticle synthesis. The reaction mixture were held at 80°C for 2 hours until pale white precipitate developed, signifying the creation of a magnesium hydroxide precursor.

The resultant precipitate was subjected to centrifugation and thoroughly rinsed with ethanol and deionized water to remove remaining contaminants. The precipitate was further dried in a hot air oven at 100°C for 12 hours and calcined in a muffle furnace at 500°C for 3 hours to produce Magnesium oxide (MgO) nanoparticles (Badilli *et al.* 2026). The generated MgO nanoparticles were finely ground with a pestle and mortar and later employed as filler reinforcement in the production of Clitoria ternatea fiber-reinforced epoxy composite laminates.

2.4 Fabrication of *Clitoria ternatea* Fiber Reinforced MgO/Epoxy Composite Laminates

Composite laminates were produced utilizing the traditional hand lay-up method with a stainless-steel mold of 300 mm × 300 mm × 5 mm. Before fabrication, the mold surface was meticulously cleaned with acetone to eliminate dust and surface impurities, then liquid wax was applied as a mold release agent to ensure effortless removal of the cured laminates. Araldite HY951 hardener and Bisphenol-F type LY556 epoxy resin were employed as matrix system. The amine-based hardener and epoxy resin were combined in a 10:1 weight ratio to ensure efficient crosslinking and consistent curing properties at ambient temperatures. The curing reaction between epoxy resin and hardener facilitated the creation of a three-dimensional crosslinked polymer network, hence improving the mechanical, thermal, and chemical resilience of the resultant composite laminates.

The required MgO nanoparticles were mechanically dispersed in the epoxy resin at 500 rpm for 15 min**.** The mixture was subsequently degassed under vacuum for 10 min to remove entrapped air. HY951 hardener was then added to LY556 epoxy resin at a 10:1 weight ratio and mixed at 300 rpm for 5 min**.** Alkali-treated fibres, cut to approximately 30 mm, were gradually introduced and uniformly distributed in layers within the mould cavity. The composite laminates were manufactured by altering the weight ratio of alkali-treated *Clitoria ternatea* fiber and green-generated MgO nanoparticles, serving as reinforcement and filler materials, respectively. The composite materials were labeled A, B, C, D, and E according to their fiber/filler weight ratios. All produced samples maintained a constant matrix composition of 70wt% comprising a blend of epoxy resin and hardener. The determined amount of green-generated MgO nanoparticles was uniformly dispersed in the epoxy matrix using mechanical stirring to reduce agglomeration and ensure even distribution within the resin system. Subsequently, chopped *Clitoria ternatea* fibers, approximately 30 mm in length were progressively integrated into the MgO-filled epoxy matrix and uniformly distributed in layers within the mold cavity. MgO agglomeration was minimized by gradually adding the nanoparticles to the epoxy resin under continuous mechanical stirring before fiber incorporation. Dispersion quality was assessed qualitatively using SEM–EDX observations.

Subsequent to laminate preparation, the manufactured composites underwent post-curing in a hot-air furnace at a regulated heating rate of 5°C/min for 120 minutes to guarantee complete polymerization and enhanced interfacial adhesion among fiber, filler, and matrix phases. A compressive force of 5 kg was uniformly applied to the laminate surface for 24 hours at room temperature to reduce void formation and enhance dimensional stability. Upon final curing, the fabricated composite laminates were meticulously demolded and sectioned in accordance with ASTM standards for subsequent characterization tests.

Table 1. Material composition of CTF-reinforced MgO/epoxy composite laminates

Specimen	CT Fiber (wt%)	MgO Filler (wt%)	Epoxy
A	29	1	70
B	28	2	70
C	27	3	70
D	26	4	70
E	25	5	70

Three independently prepared specimens (n = 3) from each composite formulation were evaluated for every mechanical and antibacterial measurement. The experimental results were obtained directly from the respective testing instruments and expressed as mean ± standard deviation. The engineered *Clitoria ternatea* fiber-reinforced MgO/epoxy composite laminates were subsequently characterized via antibacterial analysis, scanning electron microscopy with energy-dispersive X-ray spectroscopy (SEM–EDX), X-ray diffraction (XRD), Fourier transform infrared spectroscopy (FTIR), thermogravimetric analysis (TGA), tensile, flexural, and impact tests to assess their structural, morphological, thermal, biological, and mechanical performance attributes. MgO loadings of 1–5 wt.% were selected to evaluate the progressive effect of low nanoparticle concentrations on composite performance. This range was chosen because low MgO contents may improve interfacial interactions, whereas excessive loading can increase resin viscosity and promote nanoparticle agglomeration. The epoxy content and total

reinforcement were maintained at 70 and 30 wt.%, respectively, with each increase in MgO content accompanied by a corresponding reduction in fiber content.

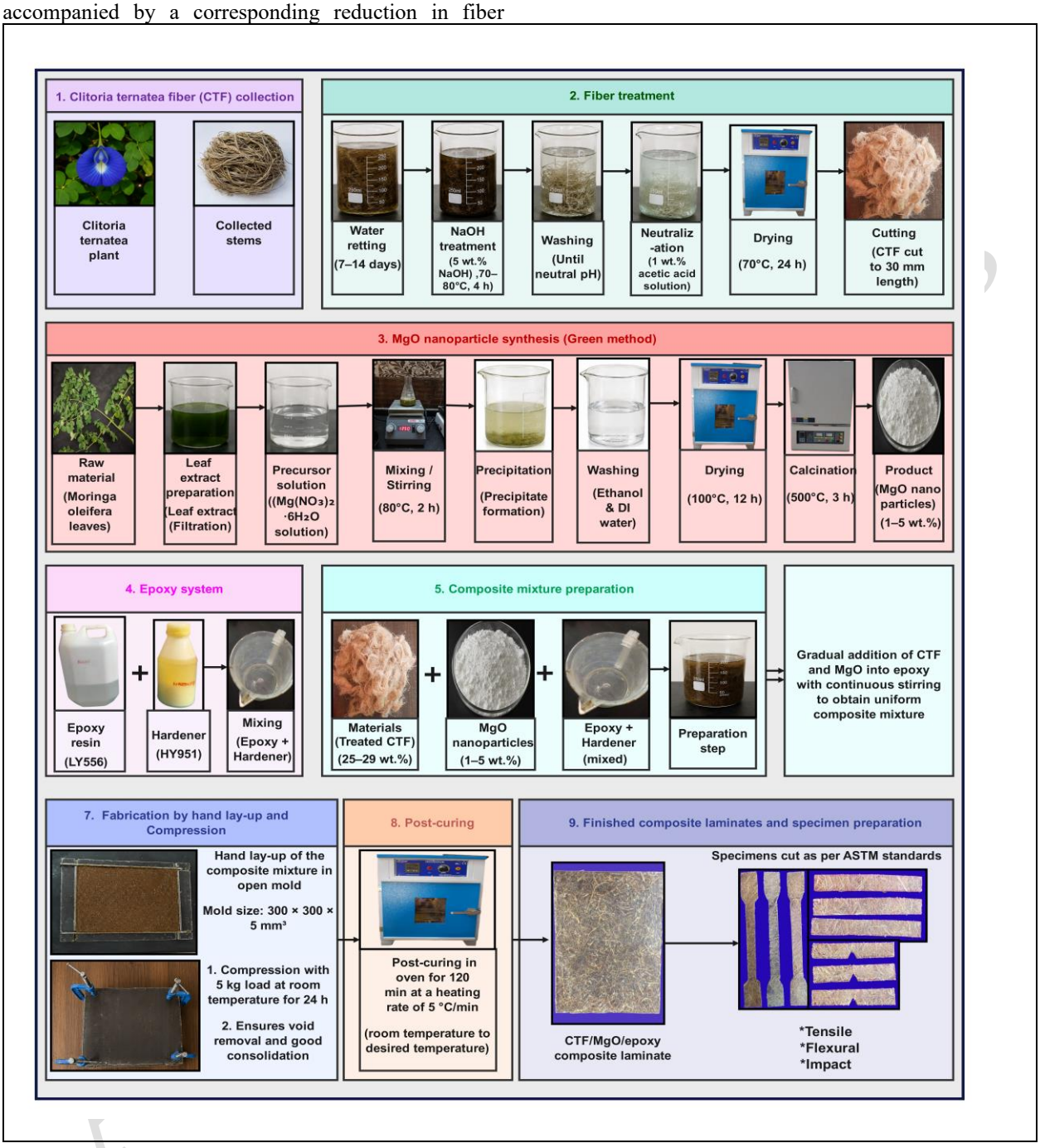

Fig. 1: Fabrication of CTF/MgO/epoxy hybrid composite

2.5 Experimental Evaluation of CTF Composite

Antibacterial activity was evaluated using the agar-disc diffusion method against two Gram-positive bacteria, *Streptococcus mutans* and *Staphylococcus aureus*, and two Gram-negative bacteria, *Klebsiella pneumoniae* and *Escherichia coli*. Fresh bacterial cultures were adjusted to the 0.5 McFarland standard, corresponding to approximately 1.5×108 CFU mL^{-1}, and uniformly inoculated onto Mueller–Hinton agar plates. Sterilized Sample D composite discs were placed on the inoculated agar surface. Erythromycin and amoxicillin discs served as positive controls, while a sterile blank disc served as the negative control. The plates were incubated at 37±1 ∘C for 24 h. Antibacterial activity was determined by measuring the inhibition-zone diameter in millimetres. Each experiment was conducted in triplicate (n=3), and the average inhibition-zone value was

reported. No inferential statistical analysis was performed; the results were evaluated descriptively using the experimentally measured inhibition zones. This evaluation was conducted as a preliminary assessment of the antibacterial functionality of the developed composite and its potential relevance to antimicrobial surface applications. The test was not intended to establish biomedical suitability because cytocompatibility, toxicity, bioactivity, and in vivo performance were not evaluated in the present study. The composite laminates were structurally characterized using X-ray diffraction analysis in accordance with ASTM standards to ascertain crystalline structure, phase composition, and crystallinity of the created material system. Furthermore, Fourier Transform Infrared Spectroscopy examination was performed in accordance with ASTM E168 to ascertain functional groups and chemical interactions inside the composite laminates. Additionally, mechanical characterisation of the produced composites was conducted to assess their appropriateness for polymer matrix composite applications under various loading circumstances.

The mechanical evaluation of the produced composite laminates was conducted in accordance with ASTM standards to guarantee testing reliability and dimensional uniformity among samples A–E. Tensile characteristics were assessed utilizing an Instron Universal Testing Machine following ASTM D638 standards with a crosshead speed of 2 mm/min and a load capacity of 40 kN. The tensile specimens were fabricated by dimensions of 150 × 12 × 3 mm^3. Flexural behavior of composites was assessed in accordance with ASTM D790 standards, utilizing samples of 120 × 12 × 3mm3 with a span-to-depth ratio of 100:1. The impact resistance of fabricated laminates was assessed in accordance with the ASTM D256 standard, utilizing samples measuring 75 × 12 × 3 mm^3. Fiber dispersion, surface morphology, interfacial adhesion, and fracture characteristics of hybrid composites were examined utilizing a ZEISS Gemini scanning electron microscope (SEM). Before microscopic investigation, the specimen surfaces were sputter-coated with silver particles for 116 seconds to enhance conductivity and image clarity during surface microstructural analysis. Degradation characteristics and thermal stability of composite laminates were assessed by thermogravimetric analysis in accordance with ASTM E1131 standards. About 15 mg of the composite sample was subjected to heating from room temperature to 500°C at a regulated rate of 5°C/min utilizing a TGA 2950 apparatus to assess the thermal decomposition properties and mass loss behavior of the material system. X-ray diffraction analysis was performed using Cu Kα radiation (λ = 1.5406 Å) at 40 kV and 30 mA over a 2θ range of 10–80° with a scan rate of 2° min^{-1}. This study selected sample D for antibacterial, XRD, and FTIR investigations due to its optimum fiber-filler interaction, superior structural stability, and greater compatibility among *Clitoria ternatea* fiber, MgO nanoparticles, and the epoxy matrix system. Nonetheless, SEM, TGA, tensile, flexural, and impact assessments were conducted on all manufactured composite samples (A–E) to comparatively analyze their overall mechanical, thermal, and morphological performance attributes. A two-stage evaluation procedure was adopted. First, all composite formulations (A–E) were evaluated through tensile, flexural, impact, SEM, and TGA analyses. The formulation exhibiting the highest combined mechanical performance was then selected for detailed XRD, FTIR, and antibacterial analyses. Before mechanical testing, all specimens were conditioned at 23 ± 2 °C and 50 ± 5% relative humidity for 40 h. Tensile, flexural, and impact tests were then performed under the same controlled environmental conditions. Three specimens (n = 3) from each composite formulation were tested for each mechanical property, and the results were reported as mean ± standard deviation. Sample D was selected because it recorded the highest tensile strength (42.1 MPa), flexural strength (43.2 MPa), and impact energy (11.0 J) among the investigated formulations. Thus, its selection was based on quantitative mechanical screening rather than subjective observation.

3. RESULTS AND DISCUSSION

The hybrid composite, reinforced with *Clitoria ternatea* fiber and an epoxy matrix loaded with Magnesium Oxide (MgO) nanoparticles, was methodically examined to assess its structural, biological, mechanical, thermal, and morphological performance attributes. The integration of MgO nanoparticles into a natural fiber-reinforced polymer matrix markedly affected the composite's overall performance, and the resulting laminates underwent a range of experimental characterization methods to evaluate their multifunctional properties and potential applications.

3.1 Antibacterial Activity of CTF Composite

The antibacterial efficacy of the *Clitoria ternatea* fiber-reinforced composite was examined to assess its capacity to impede the growth and proliferation of pathogenic microorganisms. The observed antibacterial activity indicates the material's potential for further investigation. However, its practical or biomedical suitability cannot be established without biological safety, durability, and application-specific evaluations.

Sample D of the *Clitoria ternatea* fiber-reinforced composite was chosen for the antibacterial investigation due to its optimal fiber-filler compatibility, improved structural stability, and superior mechanical performance relative to the other manufactured laminates. The antibacterial efficacy of the composite was assessed against four bacterial strains, including two Gram-positive bacteria, Streptococcus mutans and

Staphylococcus aureus, and two Gram-negative bacteria, *Klebsiella pneumoniae* and *Escherichia coli*. Erythromycin and Amoxicillin, each at a dosage of 10 mg, were employed as reference standards for the analysis of Gram-positive and Gram-negative bacteria. Experimental outcomes validated that the synthesized composite exhibited substantial antibacterial efficacy relative to traditional antibiotics. Composite exhibited inhibitory zones of 15.3 mm for *Streptococcus mutans*, 18.1 mm for *Staphylococcus aureus,* 14.8 mm for *Klebsiella pneumoniae* and 16.9 mm for *Escherichia coli*. In prior studies, antibacterial testing revealed that MgO- and ZnO-loaded hydrogel nanocomposites exhibited the strongest antimicrobial activity against *P. mirabilis*, *S. aureus*, *P. aeruginosa*, and *C. albicans*. The MgO-hydrogel reduced *S. aureus* growth by 68.89% and showed the lowest OD600 value (0.896), indicating superior antibacterial effectiveness (El Fadl *et al.* 2023). The inherent susceptibility of natural fibers to microbial destruction due to their organic makeup necessitates the integration of antibacterial properties, which markedly enhances the durability, cleanliness, and longevity of the composite material. The observed antibacterial activity indicates that the developed composite may be considered for further investigation in hygienic and antimicrobial surface applications. However, direct biomedical use cannot be established from inhibition-zone measurements alone, and additional cytocompatibility, toxicity, durability, and application-specific biological evaluations are required. The comprehensive antibacterial performance findings of the fabricated composite laminates are displayed in Table 2.

Table 2. Antibacterial activity of CTF composite

Bacterial Strain	Sample D Zone (mm)	Positive Control	Disc Potency (µg disc^{-1})	Positive-Control Zone (mm)	Negative-Control Zone (mm)
Klebsiella pneumoniae	14.8	Amoxicillin	10	10	0
Escherichia coli	16.9	Amoxicillin	10	10	0
Streptococcus mutans	15.3	Erythromycin	15	12	0
Staphylococcus aureus	18.1	Erythromycin	15	10	0

The antibacterial activity may arise from surface-exposed MgO nanoparticles interacting with bacterial cell walls, causing membrane disruption and leakage of intracellular components. MgO surface defects may also generate reactive oxygen species, including $O_2^{\bullet-}$, •OH, and H_2O_2, which can damage membrane lipids, proteins, and DNA. However, these mechanisms were not directly evaluated; therefore, they are proposed based on previous literature.

3.2 X-ray Diffraction of CTF Composite

XRD investigation of *Clitoria ternatea* fiber-reinforced composite identified distinct diffraction peaks associated with the cellulose crystalline planes (110), (200), and (004) at roughly 2θ values. XRD characterisation was extensively utilized to examine crystalline properties, phase identification, and structural configuration of natural fiber composites. The diffraction pattern from sample D was studied to assess crystallinity and phase composition of the generated composite system. Distinct diffraction peaks were observed at 2θ values of 15.8°, 22.4°, and 34.6°, corresponding to cellulose crystalline planes (110), (200), and (004), respectively, based on ICDD PDF No. 00-060-1502. Furthermore, characteristic MgO diffraction peaks were identified at 36.8°, 42.9°, and 62.3°, corresponding to the (111), (200), and (220) crystallographic planes consistent with JCPDS/ICDD PDF No. 45-0946. The broad diffraction hump observed between approximately 12° and 25° indicated the presence of the amorphous epoxy matrix within the composite structure. The coexistence of cellulose and MgO diffraction peaks confirmed successful addition of MgO nanoparticles within the epoxy matrix, while the amorphous hump reflected the polymeric nature of the epoxy phase. Enhanced crystallinity in polymer composites typically results in superior tensile strength, stiffness, impact resistance, and dimensional stability, hence augmenting the material's appropriateness for structural engineering applications. Moreover, composites exhibiting enhanced crystalline properties demonstrate greater thermal resistance and endure higher temperatures with diminished thermal degradation. Natural fibers possess inherent hydrophilic properties that facilitate moisture absorption; thus, an increase in crystallinity contributes to the reduction of water uptake by diminishing the composite system's hydrophilicity. Thus, enhanced crystallinity improves the structural durability and environmental resistance of composite materials. Crystalline properties and structural features of manufactured composite laminates were depicted in the XRD pattern, as shown in Fig. 2. According to earlier studies, XRD confirmed successful formation of crystalline ZnO nanoparticles synthesized using *Clitoria ternatea* flower extract. The diffraction peaks corresponded to the characteristic crystal structure of ZnO, indicating high purity and good crystallinity of the nanoparticles (Dadsena *et al.* 2025).

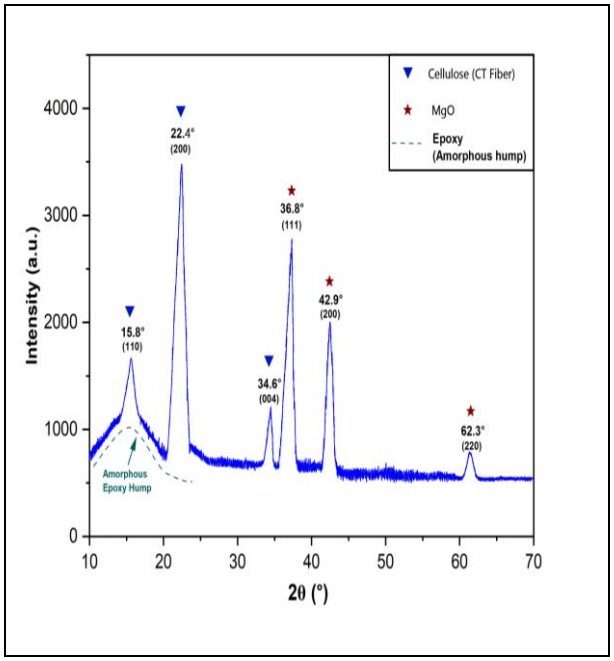

Fig. 2: XRD pattern of optimized composite (sample D)

The improvement in crystallinity was primarily due to the addition of nanoparticle reinforcement, which facilitated better structural ordering in the polymer matrix, while the amorphous regions enhanced interfacial bonding between the reinforcing fiber and matrix phases.

The apparent crystallinity index was determined using the XRD peak-area integration method after background correction. The integrated areas of the fitted cellulose and MgO crystalline peaks were considered the total crystalline area (A_c), whereas the integrated area of the broad epoxy-associated amorphous halo was considered the amorphous area (A_a). The apparent crystallinity index and amorphous fraction were calculated using Eqs. (3) and (4), respectively:

$$CI(\%) = \frac{A_c}{A_c + A_a} \times 100 \quad \ldots (3)$$

$$AF(\%) = \frac{A_a}{A_c + A_a} \times 100 = 100 - CI \quad \ldots (4)$$

where A_c represents the combined integrated area of the crystalline cellulose and MgO peaks, and A_a represents the integrated area of the amorphous epoxy halo. Because the composite contains crystalline MgO, cellulose and amorphous epoxy phases, the calculated value represents the apparent crystallinity of the overall composite rather than the absolute crystallinity of cellulose alone.

The crystallinity index of the optimized composite was approximately 74%, while the amorphous fraction was 26%, indicating a predominantly crystalline structure.

3.3 FTIR Analysis of CTF Composite

Fourier Transform Infrared Spectroscopy were prevalent analytical method employed in the investigation of both organic and inorganic materials to identify chemical functional groups and molecular interactions within a material system. The approach functions by assessing the vibrational frequencies of atomic bonds under infrared radiation, facilitating the identification of diverse chemical components inside the composite structure. This work conducted FTIR analysis of the *Clitoria ternatea* fiber-reinforced composite to examine its chemical composition, interfacial bonding properties, and distribution of functional groups. The acquired FTIR spectrum displayed several characteristic absorption peaks associated with cellulose, lignin, epoxy matrix constituents, and MgO nanoparticles. A broad absorption band at 3340 cm^{-1} was attributed to O–H stretching vibrations, indicating possible hydrogen bonding among cellulose, cured epoxy, and surface hydroxyl groups of MgO and absorbed moisture, while the peak at 2924 cm^{-1} corresponded to C–H stretching vibrations. The absorption band at 1730 cm^{-1} was assigned to C=O stretching vibrations, whereas the peak at 1605 cm^{-1} represented aromatic C=C stretching of the epoxy matrix. The band observed at 1510 cm^{-1} was associated with aromatic ring vibrations. Furthermore, the peaks at 1245 cm^{-1} and 1160 cm^{-1} and the Mg–O band at 600 cm^{-1} corresponded to C–O–C stretching vibrations; the peak at 1030 cm^{-1} was attributed to C–O stretching of polysaccharide constituents. Absorption band at 897 cm^{-1} were assigned to β-glycosidic linkages present in cellulose. In addition, the characteristic peak observed at 600 cm^{-1} confirmed presence of Mg–O stretching vibrations, indicating the successful incorporation of MgO nanoparticles within composite matrix. Minor peaks detected in the spectrum may also result from the presence of pectin, waxes, and extractive chemicals inherent in the fiber structure. Fluctuations in peak intensity, peak position, and spectral morphology were affected by fiber treatment, composite manufacturing circumstances, and chemical interactions among the fiber, MgO nanoparticles, and epoxy matrix. The fingerprint region below 1500 cm^{-1} provided significant information regarding the presence of C–O, C–O–C, and β-glycosidic functional groups within the fabricated composite system. The detected spectral changes validated the presence of intermolecular interactions and improved bonding characteristics in the produced composite laminates. Figure 3 displays the FTIR spectrum of the produced composite material. Several researchers have examined FTIR analysis, confirming the inclusion of various bioactive functional groups derived from *Clitoria ternatea* extract on the surface of synthesized iron oxide nanoparticles. These functional groups acted as stabilizing and reducing agents, facilitating nanoparticle formation and enhancing their stability (Kachhawaha *et al.* 2025).

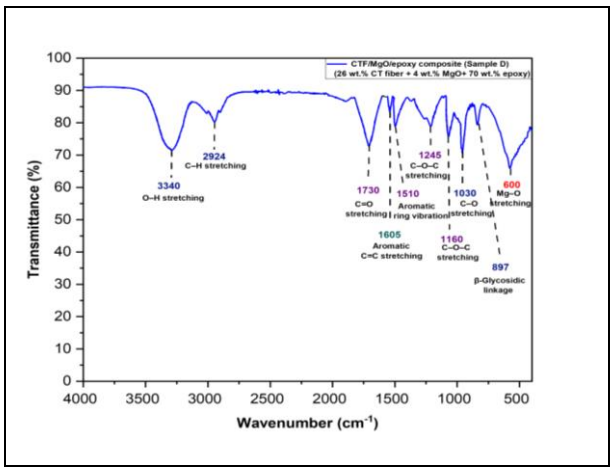

Fig. 3: FTIR spectrum of optimized composite (sample D)

3.4 Mechanical Performance of CTF Composites

The hybrid composite was developed using *Clitoria ternatea* fibres as the primary reinforcement and the epoxy as the matrix material, with the addition of Magnesium Oxide (MgO) nanoparticles as filler. The epoxy resin in the composite system was the glue that united the reinforcing fibers and filler particles together, forming a composite laminate. Incorporating natural CT fibers significantly improved load-bearing capacity and overall mechanical properties of the composite, particularly flexural resistance, tensile strength and impact energy absorption. The synergistic effect between fiber reinforcement, MgO nanoparticles and the epoxy matrix enhanced the structural performance of the fabricated laminates. Mechanical properties of composite samples were shown in Fig. 4. For each composite formulation (A–E), three independent specimens (n = 3) were tested for tensile strength, flexural strength, and impact energy. Thus, 15 specimens were evaluated for each property and 45 specimens overall.

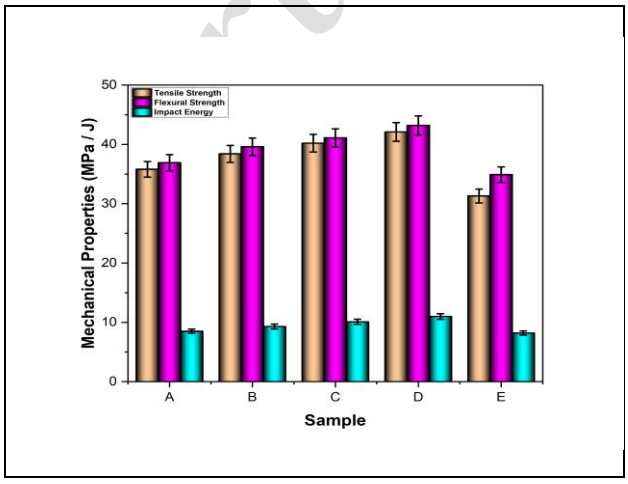

Fig. 4: Mechanical properties of CTF/MgO/epoxy composites (sample D)

Tensile strength of the fabricated composite laminate samples (A-E) was in the range of 31.3 MPa to 42.1 MPa. Natural fibers contain non-cellulosic material like lignin, wax, and hemicellulose, which may negatively influence the bonding between fiber and matrix as well as the mechanical properties of the composite material. The highest tensile strength of 42.1 MPa was obtained for sample D, which has an optimal distribution of the CT fibers and MgO nanoparticles in the epoxy matrix among all manufactured specimens. The primary reason for the improved tensile properties was the efficient stress transfer mechanism that the fiber reinforcement provided, such that the loading under tensile conditions could be distributed evenly throughout the composite structure. On the other hand, the lowest tensile strength was obtained for sample E with 31.3 MPa, due to the increased matrix cracking and stress concentration, which reduced the laminate load-carrying ability. Therefore, improving the fiber extraction method to yield longer CT fibres exceeding 50 cm could further enhance the tensile performance and light load-carrying capacity of the proposed composite system under mechanical loading conditions. Earlier research suggests that the tensile strength results revealed that incorporation of MgO nanoparticles significantly enhanced the mechanical performance of the composite. Tensile strength increased from 5.31 MPa for neat epoxy to a maximum of 25.6 MPa for the MgO-reinforced nanocomposite, demonstrating the effective reinforcing action of uniformly dispersed MgO nanoparticles (Archana *et al.* 2026).

The flexural properties of manufactured *Clitoria ternatea* fiber-reinforced composite laminates were evaluated by a three-point bending test to investigate the bending resistance and bending failure nature of the manufactured composite laminates. The flexural strength of the fabricated composites ranged from 34.9 MPa to 43.2 MPa, with Sample D exhibiting the highest flexural strength owing to improved fiber–matrix adhesion and optimum MgO nanoparticle dispersion. Prior studies indicate that the flexural strength demonstrated that nettle fiber-reinforced MgO nanoparticle-filled epoxy composite exhibited enhanced bending resistance, achieving a maximum FS of 40.13 MPa. The increase was attributed to effective stress transfer among the epoxy matrix, nettle fibers, and uniformly dispersed MgO nanoparticles (Raja *et al.* 2025).

Furthermore, the fabricated laminates were found to have a better capacity for abrupt load absorption than conventional sisal fiber composites. Although, all the samples showed good impact loading resistance, sample D had the highest impact energy absorbed due to its optimum reinforcement distribution and better structural integrity. The impact energy absorption capacity ranged from 8.2 J to 11.0 J, with Sample D demonstrating the highest impact resistance due to its

superior structural integrity and efficient stress dissipation capability. Natural fiber composites have a significant dependence on a range of parameters which determine the impact resistance of the composite. This includes fiber type, reinforcement orientation, matrix properties, composite formulation and fabrication methods. The impact energy absorption capacity of natural fiber composites was generally lower than high-performance synthetic composites such as Kevlar and carbon fiber systems, but it is still capable of providing sufficient impact energy absorption for lightweight and sustainable engineering applications. Sample D exhibited the highest tensile strength, flexural strength and impact energy among the investigated composites. This behaviour may be associated with the combined effects of fibre content, MgO loading and stress transfer within the epoxy matrix. However, improved fibre–matrix interfacial bonding and uniform MgO dispersion were not directly confirmed because interfacial-strength testing, elemental mapping and quantitative fracture-surface analysis were not performed. Therefore, these mechanisms are presented only as possible interpretations of the observed mechanical behaviour.

3.5 Morphological Characterization of CTF Composites

Scanning Electron Microscopy was employed to examine the morphology and fracture characteristics of the optimized CTF/MgO/epoxy composite (Sample D). The SEM micrographs revealed rough fibrillar surfaces, fiber bundles, and matrix-covered regions, confirming the successful incorporation of *Clitoria ternatea* fibers within the epoxy matrix. The fractured surface exhibited fiber breakage, fiber pull-out, localized interfacial debonding, and crack propagation, indicating the primary failure mechanisms during mechanical loading. The rough fiber surface and fibrillar network promoted mechanical interlocking and increased stress transfer between fiber and matrix phases. Although localized fiber clustering was observed, the overall morphology suggested reasonably good fiber dispersion and fiber–matrix interaction. These morphological features are consistent with the improved tensile, flexural, and impact properties exhibited by sample D. The observed morphological features confirmed the effective reinforcing behavior of *Clitoria ternatea* fibers within the MgO/epoxy matrix and supported the enhanced mechanical performance of the optimized composite. Figure 5 illustrates the SEM morphology of the fabricated CTF/MgO/epoxy composite (Sample D). In previous studies, SEM analysis revealed that the synthesized MgO nanoparticles possessed an agglomerated and porous surface morphology, indicating successful nanoparticle formation. The porous structure provides a higher surface area and improved reactivity, which contributes to their favorable interaction with biological and environmental systems (Lavanya and Namasivayam, 2025).

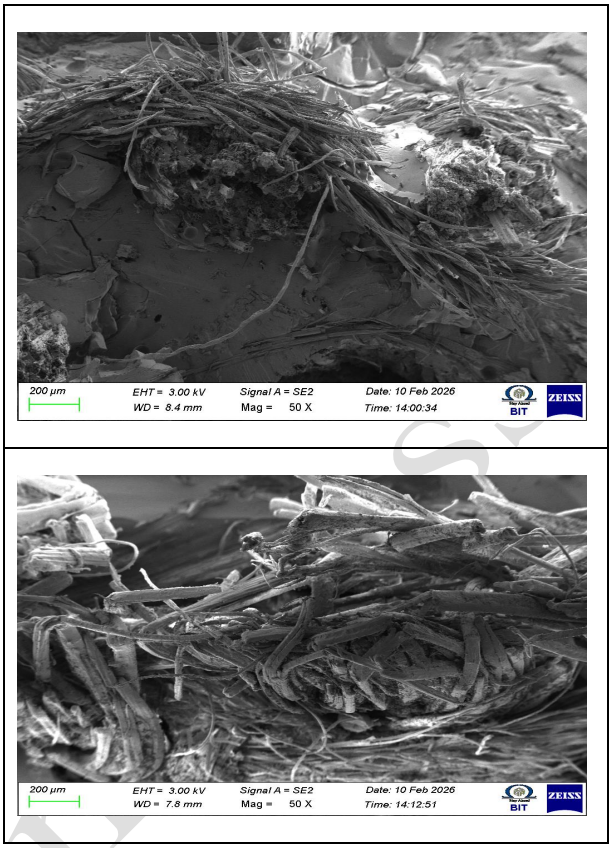

Fig. 5: SEM morphology of the optimized composite

Energy-Dispersive X-ray Spectroscopy was performed to determine the elemental composition of the fabricated Clitoria ternatea fiber-reinforced MgO/epoxy composite (Sample D). The EDX spectrum revealed the presence of carbon (C), oxygen (O), magnesium (Mg), nitrogen (N), and trace sodium (Na), confirming successful addition of MgO nanoparticles within the composite matrix. Quantitative analysis indicated elemental concentrations of 56.21 wt.% carbon, 27.45 wt.% oxygen, and 14.72 wt.% magnesium. The high carbon and oxygen contents were primarily attributed to the lignocellulosic *Clitoria ternatea* fibers and epoxy matrix, whereas the magnesium peak confirmed the presence of MgO nanoparticle reinforcement. Minor amounts of nitrogen and sodium were also detected, with the sodium peak likely originating from residual NaOH used during alkali treatment of the fibers. The EDX results verified the elemental composition of the fabricated composite and supported the successful integration of MgO nanoparticles within the epoxy-based composite system. The elemental composition profile obtained from EDX analysis is presented in Fig. 6. Earlier investigations revealed that the EDX analysis confirmed the presence of magnesium and oxygen, verifying successful synthesis of phyto-MgO nanostructures. The absence of significant impurity peaks indicated high purity and effective green synthesis (Sreevidya *et al.* 2024).

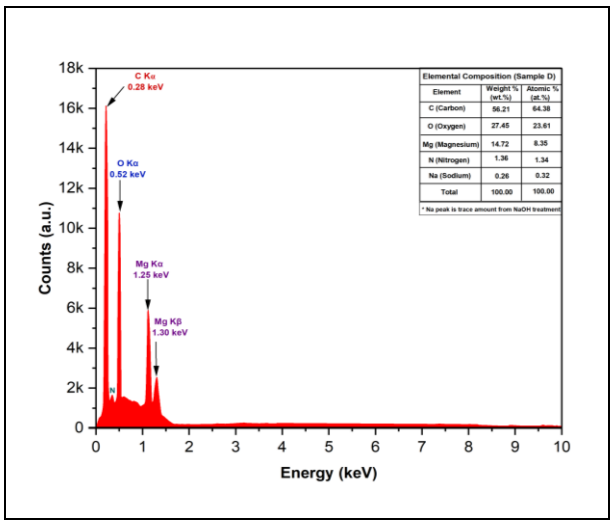

Fig. 6: EDX spectrum of the optimized composite (sample D)

3.6 Thermal Degradation Behavior of CTF Composites

Thermogravimetric analysis was employed to investigate thermal degradation behavior and thermal stability of the fabricated Clitoria ternatea fiber-reinforced MgO/epoxy composite (Sample D). The TGA technique measures the variation in sample weight as a function of temperature, thereby providing valuable information regarding the thermal decomposition characteristics of the composite system. The TGA curve revealed a multi-stage degradation behavior. The initial weight loss observed below 120°C was attributed to the removal of absorbed moisture and volatile constituents present in the natural fibers. The onset degradation temperature (Tonset) was observed at approximately 268°C, indicating the beginning of significant thermal decomposition. The second degradation stage occurring between 250°C and 380°C corresponded to the decomposition of cellulose, hemicellulose, and other lignocellulosic constituents of the *Clitoria ternatea* fibers. A major degradation stage was subsequently observed between 380°C and 520°C, which was primarily associated with thermal decomposition of the epoxy matrix. The degradation process was substantially completed at approximately 528°C (Toffset), after which a stable char residue remained. The composite retained approximately 21.4 wt.% residue at 800°C, indicating enhanced thermal stability due to the presence of MgO nanoparticles. The thermogravimetric characteristics of the fabricated composite were presented in Fig. 7(a). The DTG curve shown in Fig. 7(b) provided further insight into the degradation kinetics of the composite. A minor degradation peak was observed at approximately 110°C, corresponding to moisture evaporation. The second degradation peak appearing near 320°C was associated with the decomposition of cellulosic constituents within the fiber reinforcement. The maximum degradation rate occurred at 392°C (Tmax), corresponding to the principal degradation stage of the epoxy-rich composite structure. The TGA–DTG profile of Sample D showed moisture loss below 120 °C, lignocellulosic degradation between 250 and 380 °C, and epoxy-matrix decomposition between 380 and 520 °C. The measured T_{onset}, T_{max}, and T_{offset} values were approximately 268, 392, and 528 °C, respectively, while the residual mass at 800 °C was 21.4 wt.%. The delayed thermal decomposition and increased char formation confirmed the beneficial contribution of MgO nanoparticles toward improving the thermal stability of the fabricated composite. Earlier studies demonstrated that the addition of MgO nanoparticles significantly improved the thermal stability of biodegradable films by enhancing their resistance to thermal degradation. The increased heat resistance and delayed decomposition indicate improved thermal robustness of the matrix (Mohamad *et al.* 2023).

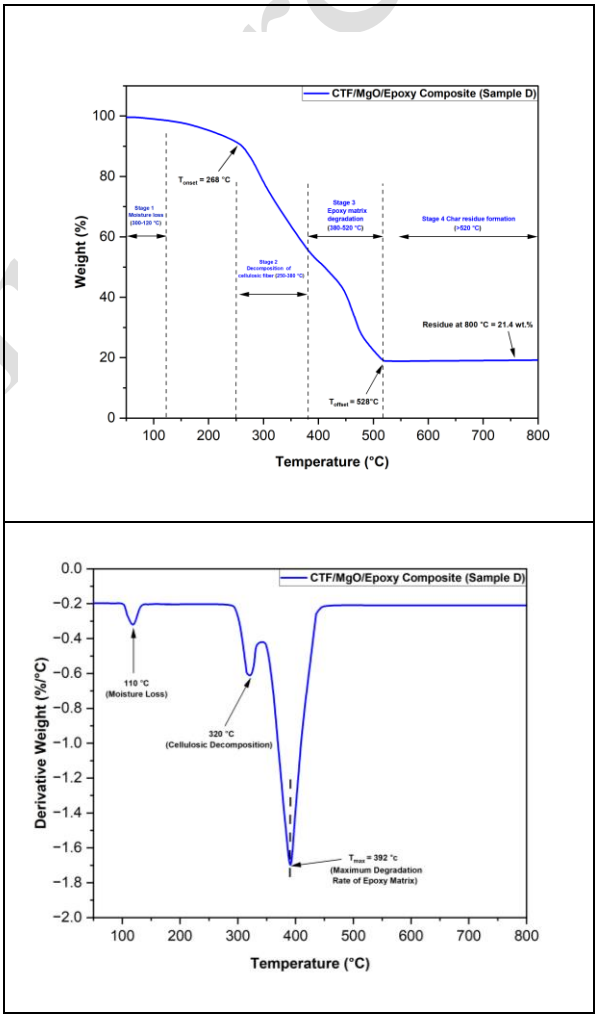

Fig. 7: TGA/DTG thermal degradation profile of the optimized composite

4. CONCLUSIONS

This study effectively manufactured and analyzed environmentally sustainable hybrid composites

reinforced with alkali-treated *Clitoria ternatea* fiber and green-generated magnesium oxide nanoparticles for biomedical and lightweight structural applications. The integration of chemically modified natural fibers and bio-synthesized MgO nanoparticles markedly enhanced the interfacial adhesion, structural robustness, antibacterial efficacy, and mechanical properties of the formulated epoxy composites. Sample D exhibited the highest combined mechanical performance, possibly due to balanced fibre reinforcement and MgO loading. Higher loading may promote agglomeration and stress concentration; however, these mechanisms require direct experimental confirmation. The antibacterial study demonstrated efficient bacterial suppression against gram-positive and negative pathogens, suggesting the composite's potential applicability in hygienic and biomedical fields. FTIR and XRD analyses confirmed presence of cellulose crystalline phases, MgO nanoparticles, and effective chemical interactions among the reinforcement, filler, and epoxy matrix. SEM investigation revealed rough fibrillar surfaces, fiber pull-out features, matrix deformation, and reasonably good fiber–matrix interaction within the composite structure. Mechanical testing revealed that, the optimized composite attained a maximum tensile strength of 42.1 MPa, a flexural strength of 43.2 MPa, and an impact strength of 11 J, attributable to efficient stress transfer and improved load-bearing capacity. Sample D produced inhibition zones of 15.3, 18.1, 14.8, and 16.9 mm against *Streptococcus mutans*, *Staphylococcus aureus*, *Klebsiella pneumoniae*, and *Escherichia coli*, respectively. Thermogravimetric analysis demonstrated a multi-stage degradation behavior with a degradation onset temperature of 268°C and a residual char content of 21.4 wt.% at 800°C, indicating improved thermal stability. The developed *Clitoria ternatea* fiber-reinforced MgO/epoxy composite demonstrates potential as a lightweight, antimicrobial, and sustainable material for structural components, protective panels, hygienic surfaces, and related engineering applications. Although antibacterial activity was demonstrated, biomedical applicability cannot yet be established because cytocompatibility, toxicity, bioactivity, biodegradability, and in vivo performance were beyond the scope of the present investigation. Subsequent research may concentrate on sophisticated surface changes, hybrid reinforcement techniques, biodegradability evaluations, and long-term durability assessments to further improve the multifunctional capabilities of the proposed composite system.

FUNDING

This research received no specific grant from any funding agency in the public, commercial, or not-for-profit sectors.

CONFLICTS OF INTEREST

The authors declare that there is no conflict of interest.

COPYRIGHT

REFERENCES

Abdullah, S. F. A., Saleh, S. S. M., Mohammad, N. F., Mahamud, S. N. S., Omar, M. F., Akil, H. M. D., Chang, B. P., Saliu, H. R., Rostam, N. H. and Gondro, J., Effect of nitrate acid treated dolomite on the tensile properties of ultra-high molecular weight polyethylene (UHMWPE) composites, *Archiv. Metall. Mater.*, 69(1), 281–288(2024). https://doi.org/10.24425/amm.2024.147820

AlZubaidi, A. A. H., Abbas, H. A. and Hassan, B. M., Comparison of Antibacterial Properties of Magnesium Oxide and Copper Oxide Nanopowders: Green Synthesis Approach, *Int. J. Adv. Sci. Eng. Inform. Technol.*, 15(1), 156–163(2025). https://doi.org/10.18517/ijaseit.15.1.12411

Amudha, K., Sampath, S., Shanmugam, D. K., Ahmed, M. Z., Alqahtani, A. S., Madav, E., Dhinakaran, M., Prakash M.V, D., Kavisri, M. and Asaithambi, P., Facile synthesis and optical characterization of selenium nanoparticles synthesized using Clitoria ternatea and Zingiber officinale: in vitro biomedical evaluation of antioxidant potential and antibacterial activity against caries-causing microbes, *Mater. Technol.*, 39(1). 2318062(2024). https://doi.org/10.1080/10667857.2024.2318062

Archana, M., Parhi, S., Ghosh, P., Datti, A. D., Narayanan, R. and Pullanchiyodan, A., Preparation of Bio-Inspired MgO-Embedded PVA-Gellan Gum Nanocomposite Films and Evaluation of In Vitro Cytocompatibility, Antioxidant, and Antibacterial Properties, *Polym. Eng. Sci.*, 66(8), 5658-5671(2026). https://doi.org/10.1002/pen.70596

Badilli, B. N., Bulut, K. B., Attar, A., Aktas, E. and Altikatoglu, Y. M., Sustainable synthesis of MgO nanoparticles from Persea americana for cultivar dependent nanostructure, environmental remediation and bioactivity supported by molecular docking, *Sci. Rep.*, 16(1), 13742(2026). https://doi.org/10.1038/s41598-026-44077-4

Dadsena, A., Narkhede, S., Singhai, A., Kolla, V., Sahu, R., Arfin, T. and Parkhey, P., Green Sythesis of Zinc Oxide Nanoparticles from Clitoria ternatea Extract:

Dual Functionality in Arsenic Adsorption and Antibacterial Applications, *Res. J. Pharm. Technol.*, 18(11), 5563–5570 (2025). https://doi.org/10.52711/0974-360X.2025.00802

Dash, P. A., Mohanty, S. and Nayak, S. K., Synthesis and characterization of ZnO/MgO doped mesoporous bioactive glass: Enhanced bioactivity and antibacterial properties for bone tissue engineering applications, *Ceram. Int.,* 51(23), 38129–38140 (2025). https://doi.org/10.1016/j.ceramint.2025.06.049

Degamon, A. L., Lavilla, M. L., Basalo, O. B., Butong, N. M. O., Cabural, D. N. P., Villarosa, M. A. M., Bendoy, A. P. and Lavilla, C. A., Combined Methanolic Extracts of Selected Medicinal Plants in Southern Philippines as a Potential Therapeutic Tool for Diabetes and Obesity, *Sci. Rise: Pharma. Sci.*, 54(2), 105–114 (2025). https://doi.org/10.15587/2519-4852.2025.328418

El Fadl, F. I. A., Hegazy, D. E., Maziad, N. A. and Ghobashy, M. M., Effect of nano-metal oxides (TiO_2, MgO, CaO, and ZnO) on antibacterial property of (PEO/PEC-co-AAm) hydrogel synthesized by gamma irradiation, *Int. J. Bio. Macromol.*, 250, 126248(2023). https://doi.org/10.1016/j.ijbiomac.2023.126248

Elkady, F. M., Alsalamah, S. A., Hashem, A., saied, E., Abdelaziz, A. M., Tawab, A. A., Salama, A., Alsenani, F., Ibrahim, N. A., Basher, N. S., Abdulrahman, M. S. and Aufy, M., Synergistic antimicrobial and antibiofilm effects of mycosynthesized MnO–MgO bimetallic nanoparticles against drug-resistant pathogens, *BMC Microbio.*, 26(1), 488(2026). https://doi.org/10.1186/s12866-026-05152-y

Fathi, A. M., Fayad, A. M., El-Beih, A. A., Taha, M. A. and Abdel-Hameed, S. A. M., Effect of ZnO addition on structure,bioactivity, and corrosion protection of mica-fluorapatite glass/glass-ceramic, *J. Austra. Ceram. Soc.*, 57(4), 1241–1253 (2021). https://doi.org/10.1007/s41779-021-00618-w

Harikrishnan, A., Purushothaman, M., Alagarasan, D., Viswanath, A. K., Pandiaraj, S., Rajabathar, J. R. and Karnan, M., A Variant Gel-Combustion Approach to Impregnate Nanostructured MgO Coating on Cotton Fibers for Antibacterial Textile Applications, *Fib. Polym.*, 24(11), 3927–3936(2023). https://doi.org/10.1007/s12221-023-00340-3

Hussain, M., Khan, S. M., Shafiq, M., Gull, N., Eladeb, A., Ghachem, K., Kolsi, L. and Khan, S. U., Comparative analysis of mechanical properties and degradation behavior in PLA composites with TCP, ZnO, MgO, and ZrO_2, *J. Thermoplast. Compos. Mater*., 39(6), 2927-2950(2025). https://doi.org/10.1177/08927057251397378

Kachhawaha, A. S., Elizabeth, M., Hari, P., Rajan, A. and Verma, N., Green Synthesis and Antibacterial Evaluation of Iron Oxide Nanoparticles using Clitoria ternatea Flowers, *Biomed. Pharmacol. J.*, 18(1), 749–759 (2025). https://doi.org/10.13005/bpj/3125

Lavanya, M. and Namasivayam, S. K. R., Eco-friendly fabrication of magnesium oxide nanoparticles from Clitoria ternatea and their influence on plant growth parameters of Vigna mungo, soil nutrient dynamics and computational analysis, *Plant Nano Bio.*, 14, 100200 (2025). https://doi.org/10.1016/j.plana.2025.100200

Mittal, V., Saini, R. and Sinha, S., Natural fiber-mediated epoxy composites–a review, *Compos. Part B: Eng.*, 99, 425-435(2016). https://doi.org/10.1016/j.compositesb.2016.06.051

Moghanian, A., Ghorbanoghli, A., Kazem-Rostami, M., Pazhouheshgar, A., Salari, E., Saghafi Yazdi, M., Alimardani, T., Jahani, H., Sharifian Jazi, F. and Tahriri, M., Novel antibacterial Cu/Mg-substituted 58S-bioglass: Synthesis, characterization and investigation of in vitro bioactivity, *Int. J. Appl. Glass Sci.*, 11(4), 685–698 (2020). https://doi.org/10.1111/ijag.14510

Mohamad, E. A., Shehata, A. M., Abobah, A. M., Kholief, A. T., Ahmed, M. A., Abdelhakeem, M. E., Dawood, N. K. and Mohammed, H. S., Chitosan-based films blended with moringa leaves and MgO nanoparticles for application in active food packaging, *Int. J. Bio. Macromol.*, 253, 127045(2023). https://doi.org/10.1016/j.ijbiomac.2023.127045

Mohanta, Y. K., Mishra, A. K., Panda, J., Chakrabartty, I., Sarma, B., Panda, S. K., Chopra, H., Zengin, G., Moloney, M. G. and Sharifi-Rad, M., Promising applications of phyto-fabricated silver nanoparticles: Recent trends in biomedicine, *Biochem. Biophys. Res. Commun.*, 688, 149126(2023). https://doi.org/10.1016/j.bbrc.2023.149126

Nadian, N., Nourouzi, S. and Jamshidi, A. H., Plasma-Sprayed HA-Ti-MgO Composite Coating for Improving Ti_6Al_4V Alloy Performance, *Eng. Rep.*, 7(10), e70452 (2025). https://doi.org/10.1002/eng2.70452

Raja, T., Devarajan, Y., Logesh, K., Rajiv, A., Jagdish Upadhye, V. and Tiwari, K., An in-depth investigation into the utilization of nettle fiber-reinforced epoxy composites with embedded MgO nanoparticles, *J. Reinforce. Plast. Compos.*, 44(23–24), 2862–2873 (2025). https://doi.org/10.1177/07316844241266650

Sarfraz, M. H., Hayat, S., Siddique, M. H., Ashraf, A., Zubair, M., Khurshid, M., Ahmed, T., Li, B., Sarfraz, M. F., Ali, B., Bach, H. and Muzammil, S., Bioinspired synthesis and characterization of chitosan-based MgO nanoparticles: Evaluating antibacterial potential against MDR pathogens and anticancer activity in HEPG2 cell lines,*International J. Bio. Macromol.*, 312, 144091(2025). https://doi.org/10.1016/j.ijbiomac.2025.144091

Shkir, M. and Ali, A. M., Enhanced antibacterial activity and photocatalytic degradation by Clitoria ternatea

flower extract-based green CeO_2 nanoneedles for wastewater and antibacterial applications, *Appl. Phys. A: Mater. Sci. Proce.*, 132(4), 244(2026). https://doi.org/10.1007/s00339-026-09358-9

Sreevidya, S., Yadav, S., Sanwaria, S., Katre, Y., Kotasthane, A., Kumar, R. S., Singh, A. K. and Susan, M. A. B. H., Phyto-nano-MgO quantum dots by ultrasonic formulation for evaluation of toxin In-Vivo/Vitro/Silico sequels, *Chem. Eng. J.*, 483, 149089(2024). https://doi.org/10.1016/j.cej.2024.149089

Wang, X., Cui, L., Fan, S., Li, X. and Liu, Y., Biodegradable poly(Butylene adipate-co-terephthalate) antibacterial nanocomposites reinforced with MgO nanoparticles, *Polym.*, 13(4), 507 (2021). https://doi.org/10.3390/polym13040507

Wang, X., Jin, H., Zhang, S., Zou, Z., Zhang, T., Lv, Y., Yuan, Z., Han, W. and Li, Q., Regulation of Mechanical Properties and Degradation Behavior of Poly(L-Lactide-Co-ε-Caprolactone) (PLCL) by Magnesium Oxide Nanoparticle, *Polym. Eng. Sci.*, 65(9), 4595–4605 (2025). https://doi.org/10.1002/pen.27279